ADVANCED FUNCTIONAL MATERIALS
www.afm-journal.de

www.MaterialsViews.com

pH-Responsive Round-Way Motions of a Smart Device through Integrating Two Types of Chemical Actuators in One Smart System

*Lingling Yu, Mengjiao Cheng, Mengmeng Song, Dequn Zhang, Meng Xiao, and Feng Shi**

Smart motions of objects from the submicrometer to millimeter scale through chemical control with stimulus-responsive way are significant to achieve various applications. However, the intelligence of the current devices with chemical responding system remains to be improved; especially, achieving a round-way motion is still a challenge. Therefore, two types of actuators are simultaneously integrated into single smart device at the opposite ends to achieve cooperated functions in an orderly manner. One actuator is the pH-responsive power supply of hydrogen bubbles produced from the reaction between magnesium and HCl. The smart device undergoes on–off–on locomotion through control over the solution pH values by using the pH-responsive actuator of magnesium–HCl system. The other actuator is the hydrogen peroxide-responsive system of oxygen bubbles generated through the decomposition of hydrogen peroxide catalyzed by platinum aggregates. When introducing hydrogen peroxide solution into the system, the generated oxygen bubbles at the opposite end of the device to push the device backward for round-way motions. For the first time, two different types of actuators are simultaneously integrated into single smart device without disturbing each other, which realize pH-responsive round-way motions of the smart device and improve the system intelligence for further applications.

1. Introduction

Motions of small objects from the submicro to millimeter scale have gained increasing attention for potential applications in microscale robotics and motors,[1–6] manipulation of cell or bacteria,[7] drug delivery,[3] directed transportation,[8] biomimicking,[5,9,10] sensing,[11] electricity generation,[12] macroscopic assembly,[13] etc. To realize these functions, there are various strategies for motions, such as the bubble propulsion system,[13,14] self-electrophoresis,[15] Marangoni effect,[16,17] external energy of magnetic,[18] electronic[19,20] or acoustic field,[21,23] and photoirradiation.[17,22] Among these strategies, bubble propulsion is widely used as a chemical power resource because it continuously supplies strong propulsion forces for efficient motions.[13,14] Until now, in most reports, the small objects experience autonomous locomotion after the movement is started until the power resource is exhausted, and it is difficult to stop and rerestart the motions at any time according to human intention. Now, there is an increasing demand to improve the intelligence of smart motions or smart systems for new functions, such as targeted drug release or therapy,[3] micromanipulation,[7] and directional delivery.[8] Therefore, there remains the challenge of promoting the motions of small objects from an autonomous manner to controlled locomotion that responds to a stimulus, particularly responsive on/off motions.

Generally, there are two types of available methods to realize stimulus-responsive smart motions with on/off control. One strategy is to use external noncontacting energy, such as magnetic,[18] acoustic field,[23] electronic,[24] photo,[17,22] and temperature,[23,25] to stop the locomotion of smart devices and restart the motions by removing the external field from the locomotion systems. In this aspect, His group has reported directed smart motions of various nano/micromotors with magnetic guidance in a flexible way through incorporating magnetic nanoparticles into the smart devices.[26] The other method is to introduce a chemical switch by triggering a power system for the motion or cutting down the power to stop the motion. In this case, Behkam and Sitti achieved an on/off motion of polystyrene beads that were propelled by bacteria by introducing copper ions to stop the bacteria flagellar motors and adding ethylenediaminetetraacetic acid to restart the motion.[7] We reported the continuous on–off–on locomotion of a smart device by integrating pH-responsive smart materials as the switch and platinum-catalyzed bubble propulsion as the power resource in a single system.[27] The pH trigger is advantageous in being independent on certain specific materials for stimulus-responsive control and thus

L. Yu, Dr. M. Cheng, M. Song, D. Zhang, M. Xiao, Prof. F. Shi
State Key Laboratory of Chemical Resource Engineering and Key Laboratory of Carbon Fiber and Functional Polymer
Ministry of Education
Beijing University of Chemical Technology
15 Beisanhuan East Road, Chaoyang District, Beijing 100029, P. R. China
E-mail: shi@mail.buct.edu.cn

DOI: 10.1002/adfm.201502447

versatile to a wide range of materials; besides, the pH change could be easily operated and monitored through common pH indicators. However, these on/off motions that are controlled by either an external field or a chemical switch are mostly one way because the propulsion power can only be generated at one end of the smart device. Until now, there have been no reports on round-way motions, which meant that the device could move from one end to the other end and then return in respond to stimulus. This could improve the intelligence of the smart motion systems by combining two types of actuators at two separate ends of the device. Herein, we realized the pH-responsive round-way motions of a smart device by integrating two types of chemical power in one smart system. The smart device mainly comprises three major parts: a superhydrophobic hull for drag reduction on the water surface,[28] magnesium as an actuator of hydrogen bubbles, and platinum as another actuator of oxygen bubbles. In the beginning, the smart device started moving forward in an acid solution because it was propelled by hydrogen bubbles, which were generated from the chemical reaction between magnesium and acid. When the pH value was adjusted to become alkaline, the motion was stopped by inhibiting the above reaction. After hydrogen peroxide was added, the smart device moved backward because the platinum-hydrogen peroxide power system was started, which led to round-way motions. Thus, the presented integration of two types of power sources acted in an orderly manner to achieve complex motions and highly improved the intelligent degree of the smart motions, which corresponded well with the proposed principle and concept of a functionally cooperating system in our previous work.[8,17,27]

2. Results and Discussion

2.1. Preparation and Characterization of the Smart Device

To demonstrate the intelligent round-way motions, we have fabricated the smart device with three components as illustrated in **Scheme 1**: a hull modified with superhydrophobic coatings, a sheet of magnesium at one end of the hull and platinum aggregates at the other end. First, a piece of copper foam was manually folded into a boat shape due to the flexible nature of the porous copper foam. Second, the copper hull was modified with superhydrophobic coatings to introduce drag reducing property by immersing it in an aqueous solution of $AgNO_3$ (20×10^{-3} M) for 15 min to obtain rough structures followed by exposing to an ethanol solution of $SH(CH_2)_{11}CH_3$ (0.5×10^{-3} M) for 10 h as a low-surface-energy coating.[29–32] Third, a piece of magnesium (10 mm × 3 mm) was attached to one end of the modified hull to act as the actuator of the device. Fourth, platinum aggregates were obtained on gold substrates by a two-step electrochemical deposition process through immersing in $HAuCl_4$ solution for 1600 s and subsequently in H_2PtCl_6 solution for 800 s. Finally, the gold substrate deposited with platinum aggregates was attached to the opposite end of the hull, which was used as the other actuator. Considering that the two actuators of magnesium and platinum could trigger the locomotion only after contacting the solution, we attached the magnesium sheet and the substrate with platinum aggregates in the way of half immersion in solution and half exposure above the aqueous phase.

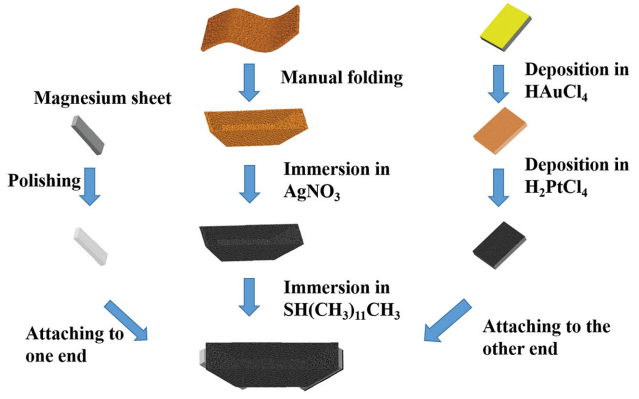

Scheme 1. Schematic illustration of fabrication process of the smart device.

In order to confirm the modification of superhydrophobic coating on the copper foam hull, we have checked both the surface morphology and wettability through scanning electronic microscopy (SEM) images and contact angle (CA) measurements, respectively. Before modification, the bare copper foam shown in **Figure 1**a exhibited a porous structure with randomly crossed meshes, which formed an average pore diameter of around 700 μm; from the corresponding local magnified SEM image in the inset, we could observe that the bare copper mesh presented a relatively smooth surface, and the major element of the foam structure was copper (energy dispersive spectrometer pattern in Figure S1a, Supporting Information). After immersed in $AgNO_3$ solution for 15 min, the copper foam displayed similar porous morphology in Figure 1b to that before modification; but the meshes were wrapped within a rough layer as indicated from the inset that the mesh was fully covered with microscale dendritic and highly branched structures in a random and crowded way. Besides, the appearance of silver element in the corresponding element pattern (Figure S1b, Supporting Information) revealed that the rough structures were attributed to the deposited silver. However, when we measured the CA of the as-prepared surface, we observed a CA value of 0° (Figure 1c). To obtain a low-surface-energy coating on the obtained silver aggregates, we modified the as-prepared substrate in an ethanol solution of $SH(CH_2)_{11}CH_3$ and observed a CA of 158.1° (Figure 1d), indicating superhydrophobicity. The transformation from superhydrophilicity to superhydrophobicity should be attributed to the formation of the self-assembled monolayer of $SH(CH_2)_{11}CH_3$,[29–32] which was confirmed by the presence of sulfur element (Figure S1c, Supporting Information). This phenomenon indicates that only the hierarchical structure with nanoscale branches on microscale scaffolds is not sufficient to realize superhydrophobicity, and the combination of a suitable surface roughness and a layer of low-surface-energy species should be necessary.[29–32] The superhydrophobic surface property of the device had plastron effect[29–32] and prevented infiltration of aqueous solution into the interior of the hull, thus creating extra empty volume within the device to provide buoyancy. For this reason, the entire device could float on the aqueous solution.

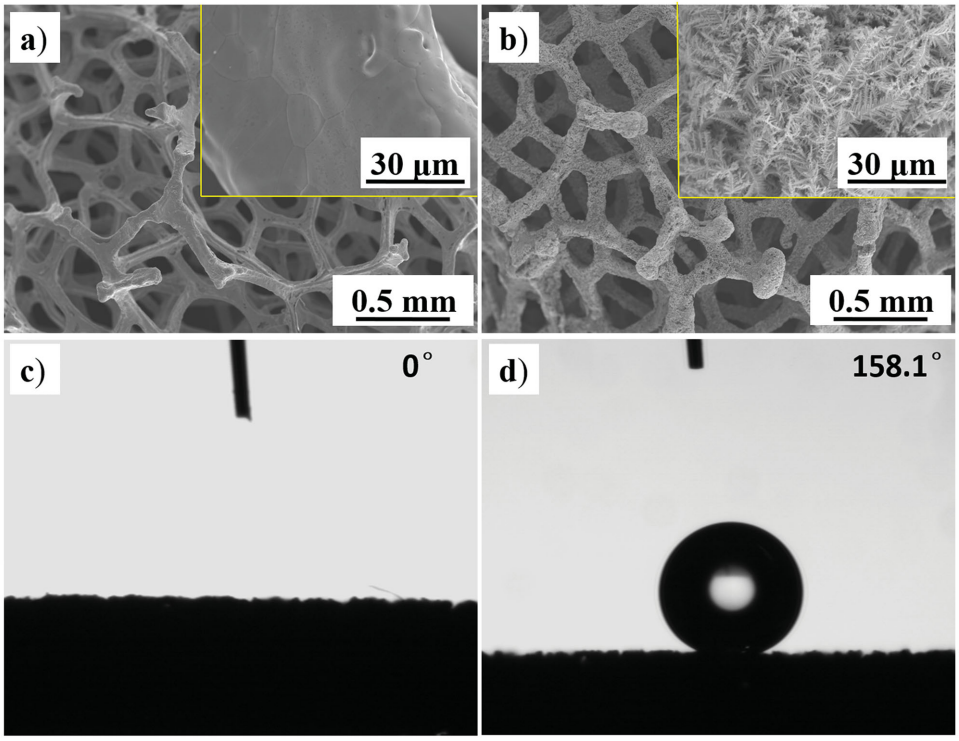

Figure 1. SEM images of a) the bare copper foam and b) the copper mesh after deposition of silver structures. Contact angle of c) the copper foam after deposition of silver structures and d) the copper mesh with the silver structures after modification with SH $(CH_2)_{11}CH_3$.

2.2. The Effects of Related Parameters on the Motion Behaviors

In order to optimize the locomotion process propelled by the actuator of magnesium in respond to acid, we have investigated the effects of related parameters (HCl concentration, device weight, and magnesium amount) on the motion behaviors, such as moving distance, moving velocity and energy consumption (**Figure 2**a–c). The moving distance versus time was recorded by tracking the position of the device with a coordination paper of parallel straight lines with a spacing of 2 cm below the glass trough; the time taken to move for a distance of 2, 4, 6, 8, and 10 cm was recorded during the locomotion of the smart device at corresponding HCl concentrations. At all volume ratios ranging from 1% to 2.5% for HCl solution, the moving distance of the device increased linearly with the reaction time, indicating a steady bubble releasing rate. The slope of the distance–time curve could be calculated to reveal the average moving velocity of the device, which increased with the growing of HCl volume ratio from 0.1 cm s^{-1} at 1% to 0.45 cm s^{-1} at 2.5% (Figure 2a, Figure S2a, Supporting Information). This result was attributed to the accelerated chemical reaction rate between magnesium and acid in a linear way when the HCl concentration was increased (Figure S2b, Supporting Information).

For the effect of the device weight, we have measured the moving velocity of the device with different loading weight by placing pieces of copper foam in the device. With the growing load weight, the moving velocity decreased correspondingly from 0.55 cm s^{-1} at a weight of 0.7 g to 0.25 cm s^{-1} at a weight of 1.0 g (Figure 2b). Because the extra loaded weight of the device contributed to more fluidic drag than that of an empty one, the moving velocity decreased with the increasing loading, which was further interpreted as follows. For the locomotion in the horizontal direction, the motion could be described by Newton's second law of motion: the vector sum of all external forces exerted on the device (F_{sum}, N) equals to the mass of the device (m, kg) multiplied by the acceleration vector (a, m s^{-2}), i.e., $F_{sum} = ma$, where $a = dv/dt = d^2x/dt^2$ (v refers to velocity, m s^{-1}; x, m is moving distance in a time interval of t, s). Ideally, when the locomotion is stationary with comparable driving force (F, N) and fluidic drag force (f, N), the acceleration value of a equals to zero and indicates a constant velocity of v. It seems that there is no relationship between the moving velocity and the device weight. However, with the increasing device weight from 0.7 to 1.0 g, the immersion depth of the centimeter scaled device increased correspondingly, which indicated extra contacting with water and thus increased fluidic drag force. In this situation, the value of $F_{sum} = F - f$ decreased due to increased fluidic drag when the chemical driving force was almost identical at a fixed HCl concentration, leading to decreased acceleration value of a. Since the acceleration value of a is linearly correlated with velocity value of v by $a = dv/dt$, the moving velocity should decrease with decreasing a value. Therefore, the increasing device weight finally contributed to decreasing moving velocity, which corresponded well with our experimental results in Figure 2b.

For the energy consumption provided by magnesium fuel, we have traced the weight change of the used magnesium sheet after immersing it in HCl solutions for different time interval. After rinsing and sufficient drying, we found that the weight

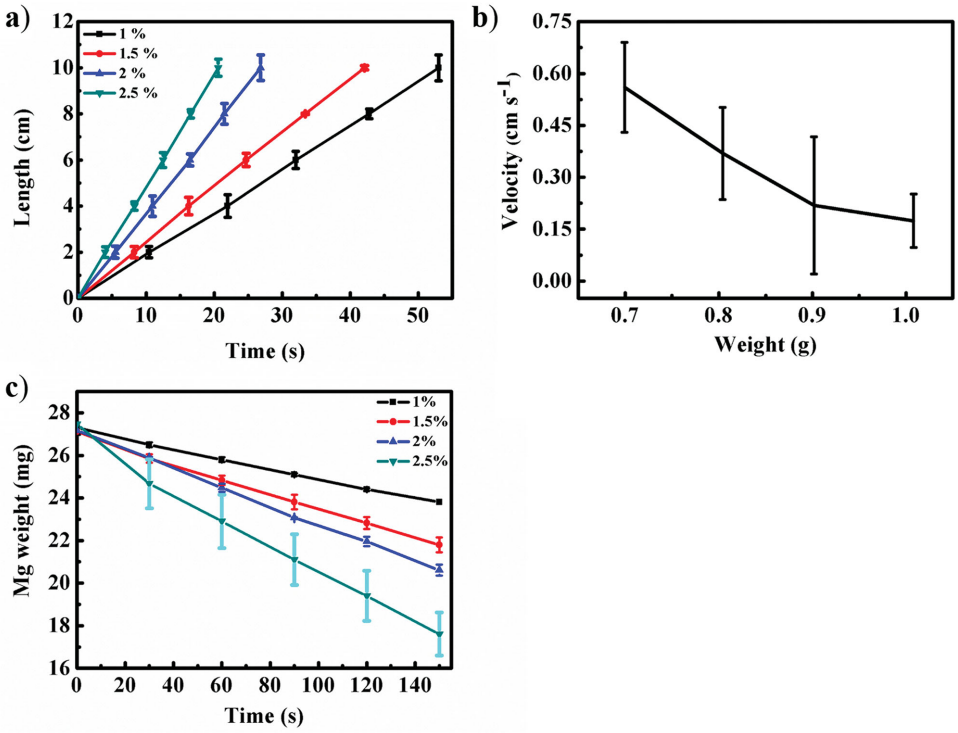

Figure 2. a) Moving distance of the smart device versus different time interval at different HCl concentrations (black cube: 1%, red circle: 1.5%, blue upper triangle: 2%, and green lower triangle: 2.5%). b) Averaged moving velocity of the smart device versus the total weight of the device. c) Weight loss of magnesium sheet versus the moving time interval (black line: 1%, red line: 1.5%, blue line: 2%, and green line: 2.5%).

loss gradually decreased with the time exposed to HCl solution, which indicated a linear magnesium consumption rate and corresponded well with the linear correlation between the moving distance and moving time as a result of steady bubble releasing from the chemical reaction. The reason for the linear weight loss of was interpreted as follows: Mg weight loss was mainly determined by two aspects, i.e., the reaction rate of magnesium and acid, and the specific area of the magnesium strip. For the reaction rate, because the factors that would affect the reaction rate such as pressure, temperature and HCl concentration kept constant, the reaction rate should be regarded as almost constant. For the specific area of magnesium, we have polished the magnesium strip with sandpaper before use and thus the magnesium surface was not rough. Therefore, the low specific area may have little influence on the reaction rate of magnesium–acid. In this way, the magnesium weight loss during the reaction with HCl was only determined by a constant reaction rate, which contributed to linearly decreased amount of magnesium. Moreover, with the increasing HCl concentration from 1% to 2.5%, the reaction rate between magnesium and HCl grew correspondingly with increasing curve slope of the magnesium weight loss versus reaction time (Figure 2c, Figure S2b, Supporting Information). Although high HCl concentration promoted rapid motions, the exerted driving forces from the bubbles on the device caused large disturbance to the device at high bubble releasing rates, which were not favorable for locomotion in a straight line; therefore, we have optimized the parameters with a HCl concentration at 1.5% and a loaded weight of 0.9 g to realize the above on–off–on motion.

2.3. On–Off–On Motion

After we have fabricated the smart device and optimized the locomotion parameters, we wondered whether we could realize its smart on–off–on motion through the pH responsive control over the hydrogen bubble generation from the reaction between the attached magnesium and acid, as illustrated in **Figure 3**a. The locomotion was carried out in a glass trough with dimensions of 2.6 cm × 1.3 cm × 1 cm, which contained hydrochloric acid (volume ratio of 1.5%) dyed with litmus (2 mL) to a red color (pH 1); the litmus indicator displayed red color below pH 4.5 and blue color above pH 8.3 and in the pH range of 4.5–8.3, it had a pH-responsive color change. Upon putting the as-prepared device (about 0.9 g) onto hydrochloric acid contained in the trough, we could observe bubble releasing from the end of the device that the magnesium was attached. Because the continuously generated bubbles exerted forces onto the device asymmetrically at one end, the device was propelled to move forward in the opposite direction of the magnesium actuator. As shown in Figure 3b-1 and Movie S1 (Supporting Information), the device underwent a self-propulsion to the middle of the trough, demonstrating that the power supply from the reaction of the loaded magnesium and acidic solution was sufficient for the locomotion of the as-prepared device. Although there were many strategies to realize such locomotion through bubble propulsion, it remained a challenge to stop and restart the motion in position. Here, we have adjusted the pH value of the solution with 2 mL ammonium hydroxide (25 wt%) to alkaline condition (pH 13). From

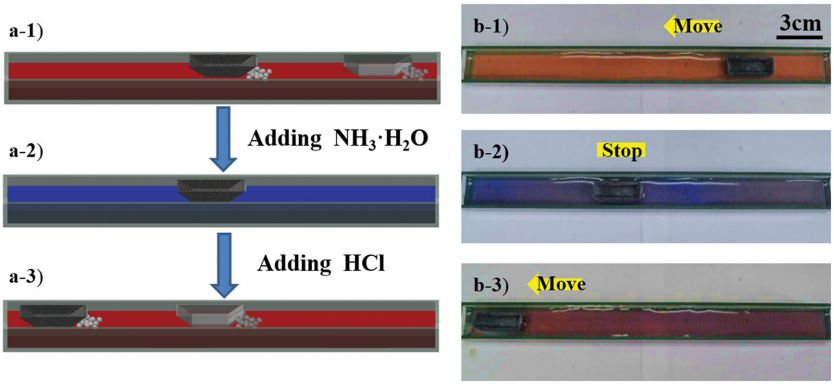

Figure 3. Illustration of the pH-responsive in position on–off–on motion of the smart device: a-1) the device starts to move in acidic solution dyed with litmus (red, pH 1); a-2) it stops after in position tuning the solution to alkaline (the solution dyed with litmus changed to blue, pH 13; a-3) after in position adjustment of the solution back to acidic (the solution color changed back to red; the pH value is about 1), the device restarts and keeps moving to the end of the trough. b-1)–b-3) are snapshots from the experiments of the in position on–off–on motion displayed in Movie S1 (Supporting Information), which correspond to a-1)–a-3), respectively.

Figure 3b-2, we could observe that after tuning to alkaline, the solution dyed with litmus changed to a blue color to indicate a high pH value and the device stopped moving forward. This phenomenon was interpreted that under alkaline condition, the reaction between magnesium and acid was inhibited and thus bubble releasing was stopped to sustain the motions. To restart the locomotion of the device for the continuous on–off–on motion (Figure 3b-3, Movie S1, Supporting Information), we have adjusted the pH value of the solution back to acidic (pH around 1) by adding 4 mL HCl (36 wt%) to the system in position, accompanied by a color change from blue to red. Although from the top view the surface was not completely red but only with some local blue color on the surface, actually the bulk solution had thoroughly changed to a red color to indicate an acidic property, as shown in Figure S3 (Supporting Information). This change occurred because the heavy HCl solution (density: 1.20 g cm^{-3}) tended to sink below water surface while the light ammonium hydroxide (density: 0.91 g cm^{-3}) was volatile to be on water surface, thus leading to insufficient mixing and neutralization between acid and alkaline on water surface. After the solution was tuned to almost acidic, the magnesium at the end of the device started reacting with acid to release hydrogen bubbles, which propelled the device forward again. In this way, the pH responsive on–off–on smart locomotion of the device was realized by triggering or inhibiting the energy supply from the chemical reaction of magnesium and acid. Compared with our previous report on pH responsive control of on/off motion,[27] in the presented method there is no need to integrate a pH-responsive smart surface into the device, thus simplifying the fabrication process of the device while maintaining the intelligence of the smart system for on/off motions.

2.4. Round-Way Locomotion

Although the motion status of on–off–on could be well tuned using pH-responsive magnesium–HCl system, there still remains a challenge to achieve round-way locomotion with in position stimulus-responsive control. The above hydrogen bubbles generated from the magnesium fuel in acid solution could only propel the device in one-way single direction, and it was difficult to alter the locomotion direction in position with the same actuator because changing the attached magnesium sheet to the other end of the device during the motion was impossible. Therefore, it is necessary to integrate another kind of stimulus-responsive actuator insensitive to pH stimuli to avoid producing disturbance to the current magnesium–HCl power source. Meanwhile this kind of power should be controllable to be start when it is required. Herein, we have introduced platinum-hydrogen peroxide system to the smart device by attaching a gold substrate modified with platinum aggregates onto the opposite end of the device. The platinum structures deposited on gold substrate displayed dendritic-like rough surfaces with hierarchical micronanostructures (Figure S4, Supporting Information). After integrated with magnesium actuator at one end and platinum actuator at the other end, the smart device could be propelled with hydrogen bubbles when the solution dyed with litmus was red to indicate acidic (pH 1, **Figure 4**b-1) and stopped when the pH was increased to alkaline condition (blue, pH 13, Figure 4b-2), leading to controlled on/off motion due to the pH responsive magnesium–acid system. To restart the motion (Figure 4b-3), we added 3 mL hydrogen peroxide solution (30 wt%) to the original system in the water trough (For the entire process, please see Movie S2, Supporting Information). The rough platinum structures at the other end of the device provided sufficient contacting with hydrogen peroxide for catalyzed decomposition to release oxygen bubbles efficiently.

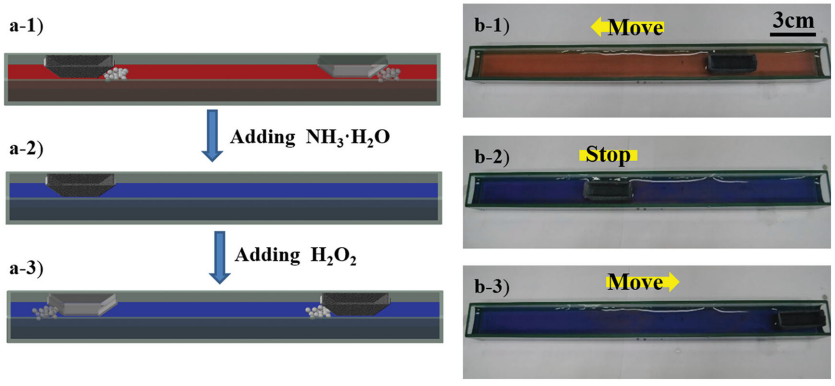

Figure 4. Illustration of the round-way locomotion of the smart device: a-1) the smart device starts to move in acidic solution indicated by litmus with a red color (pH 1); a-2) it stops when the solution was adjusted to alkaline (blue, pH 13); a-3) after adding H_2O_2, the device moved backward to the starting end. b-1)–b-3) are snapshots from the above round-way motions displayed in Movie S2 (Supporting Information), which correspond to a-1)–a-3), respectively.

In this situation, the pH value of the entire system was not changed too much to be acidic, the magnesium attached at the opposite end of the device did not react with the solution; thus the oxygen bubble propulsion system was not disturbed. Therefore, the continuously released oxygen bubbles at the platinum actuator provided propulsion force for the device to move backward, thus realizing a round-way motion. In this way, two types of actuators of magnesium–HCl and Pt-hydrogen peroxide have been integrated into the same system and act sequentially in response to pH stimuli and hydrogen peroxide, respectively, which were not disturbed with each other. Such kind of integration achieved not only smart on–off–on and round-way motions in an orderly way but also highly improved the intelligence of the smart device, contributing to the concept of functionally cooperating system.[8,17,27]

2.5. Correlation of Moving Velocity and pH Value

In order to provide comprehensive understanding of the pH-responsive control over round-way smart motions, we have investigated the correlation between the moving velocity of the smart device and pH values for both actuators of magnesium and platinum separately. For the magnesium actuator, we have fabricated the smart device only attached with magnesium sheet at one end of the device, leading to a total weight of 0.9 g. The experimental condition is similar to the on–off motion test: the as-prepared device was placed onto 100 mL of aqueous acidic solution in the glass trough; under each pH value of 0.5, 0.6, 0.7, 0.9, 1.2, 2.0, and 3.0 (for pH 0.5 ≈ 1.2, the pH values were calculated from their volume ratios of 2.5%, 2.0%, 1.5%, 1.0%, and 0.5% correspondingly), the averaged moving velocity of the device was calculated with the moving distance in a certain time interval. From the results summarized in **Figure 5**, we could observe that the moving velocity dropped dramatically from 0.45 to almost 0.1 cm s^{-1} in the pH range from 0.5 to 0.9 correspondingly; after the pH value increased to 2.0 or even 3.0, the device kept immobile with a velocity value close to zero. This phenomenon suggested that the extreme acidic condition is essential for the locomotion propelled by hydrogen bubbles release from the magnesium–acid reaction, which was remarkably inhibited when the pH value increased slightly. For the platinum actuator, we fabricated the smart device by only attaching the gold substrate deposited with platinum aggregates to one end of the hull and placed the as-prepared device onto 100 mL of hydrogen peroxide solution (volume ratio of 2.9%) contained in the glass trough. The pH value of the above system was preadjusted with NaOH solid to 5.0, 6.0, 7.0, 9.0, 11, and 13, respectively, under which the averaged moving velocity of the device in a certain time interval was calculated. As shown in Figure 5, the device kept almost immobile with a moving velocity close to zero below pH 5.0; when gradually increasing the pH value, the moving velocity presented a rapid growing to about 0.1 cm s^{-1} at pH 6.0, and reached almost 0.25 cm s^{-1} at pH 13. The results supported that the alkaline solution could increase the decomposition rate of hydrogen peroxide, thus leading to enhanced propulsion forces provided by increasing amount of oxygen bubbles released from the decomposition reaction.[27] The moving velocity curve of both the magnesium and platinum actuators was meaningful for the control of pH-responsive round-way motions of the smart device.

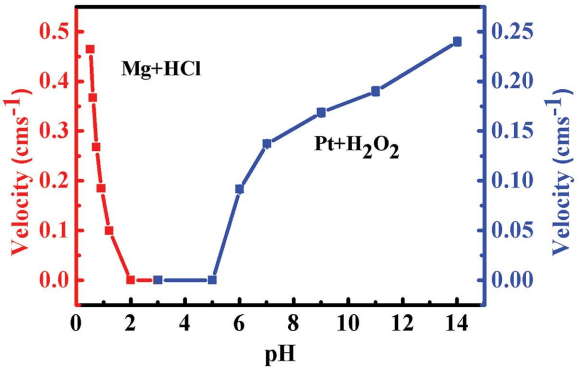

Figure 5. Correlation between moving velocity of the smart device and pH values of the solution. Red line and left *y*-axis: the smart device was only attached with the magnesium actuator; blue line and right *y*-axis: the smart device was only loaded with the platinum actuator.

3. Conclusion

To summarize, we have demonstrated pH-responsive round-way motions of a smart device through integrating two independent actuators of magnesium–acid system and platinum-hydrogen peroxide system into one smart system. The magnesium actuator could be triggered under acidic condition and inhibited in alkaline solution; correspondingly the smart device underwent on–off–on locomotion in a pH-responsive controlled way. The platinum actuator was started by introducing hydrogen peroxide into the system. With the above two actuators attached to two opposite ends of the device, the smart device could realize round-way motions adjusted through sequential triggering of the above two actuators in a functionally cooperating way. Through the concept of functionally cooperating device, we have improved the intelligence of the smart device for controlled motions, which is significant for smart motions and potential applications as cargo.

4. Experimental Section

Materials and Methods: $AgNO_3$, $NH_3{\cdot}H_2O$ (25 wt%), H_2O_2 (30 wt%), $HAuCl_4{\cdot}4H_2O$, $H_2PtCl_6{\cdot}6H_2O$, HCl (36 wt%), NaOH, litmus, and 1-dodecanethiol ($SH(CH_2)_{11}CH_3$) from Sinopharm Chemical Reagent Beijing Co., Ltd. The copper foam was purchased from AnpingXinlong Wire Mesh Manufacture Co., Ltd. The magnesium ribbon was obtained from Tianjin Fuchen Chemical Reagents Factory. Glass slides coated with a gold layer of 100 nm through evaporating gold under vacuum were obtained from Changchun institute of applied chemistry Chinese academy of sciences, which was used as gold substrate for electrochemical deposition.

Photographic images were taken with a Nikon camera (D5000). Contact angle measurement was carried out on an OCA20 instrument (Date Physics Instrument, Filderstadt, Germany). The surface morphology was characterized by SEM (Zeiss EVO MA25,

20.0 kV). Electrochemical deposition was performed on a CHI660e electrochemical workstation (Chenhua, Shanghai).

Preparation of the Smart Device: The fabrication process of the smart device is illustrated in Scheme 1. First, a piece of copper foam was cut and folded into a boat shaped device with dimensions of 2.6 cm × 1.3 cm × 1 cm, followed by cleaning in ultrasonic field with ethanol, a mixture of ethanol/deionized water (v/v = 1:1) and deionized water sequentially. Second, the device was immersed into an aqueous solution of $AgNO_3$ (0.02 M) for 15 min and then rinsed with deionized water for three times, followed by drying in oven at 70° for 2 h. Third, the as-prepared device deposited with silver was modified with low-surface-energy species by immersing in an ethanol solution of $SH(CH_2)_{11}CH_3$ for 10 h, followed by washed with copious ethanol and dried at room temperature for 3 h. Fourth, a piece of magnesium strip as pH-responsive actuator was polished with sandpaper before use. Meanwhile, the hydrogen-peroxide-responsive actuator was prepared through electrochemical deposition: a gold substrate was immersed in a mixture of H_2SO_4 (0.5 M) and $HAuCl_4$ (1 mg mL^{-1}) at –200 mV for 1600 s by taking the gold substrate as the working electrode, a platinum electrode as the counter- electrode and Ag/AgCl as the reference electrode; then the substrate was immersed in a mixture of H_2SO_4 (0.5 M) and H_2PtCl_6 (1 mg mL^{-1}) at –200 mV for 800 s. Finally, the smart device was assembled by attaching the magnesium strip (about 15 mg) at one end and the hydrogen peroxide-responsive part (about 100 mg) at the other end of the boat, leading to a total mass of 1000 ± 10 mg.

On–Off–On and Round-Way Motion of the Smart Device: The on–off–on locomotion of the as-prepared smart device with a mass of 1000 ± 10 mg was carried out in a glass trough with a dimension of 24 cm × 2.7 cm × 2.2 cm, which contained about 100 mL boiled water at about 80°. Litmus was added to act as the pH indicator with a final volume ratio of around 2%. First, the as-prepared device was placed on the water surface, and subsequently 1.5 mL of hydrochloric acid was added to the trough. Second, after the device moved about 9 cm in 35 s, the solution was adjusted to alkaline by adding 2 mL $NH_3{\cdot}H_2O$, leading to stop of motion. Third, the device was restarted by adding 4 mL hydrochloric acid. Finally, after the smart device completed the above on–off–on motion and reached the end of the trough, we added 3 mL H_2O_2 to the trough to push the device to move backward thus realizing round-way motion.

Velocity Measurements: A piece of coordinate paper was placed right below the water trough to indicate the moving distance of the smart device. As soon as the smart device started to move, we recorded the time to complete a certain distance indicated from the coordinate paper. The average velocity was calculated correspondingly at different hydrochloric acid concentrations (volume ratio: 1%, 1.5%, 2%, and 2.5%). For the velocity test, at least ten repeated measurements were carried out and the velocity was calculated with averaged values.

Supporting Information

Supporting Information is available from the Wiley Online Library or from the author.

Acknowledgements

This work was supported by National Natural Science Foundation of China (21374006 and 51422302), the Program of the Co-Construction with Beijing Municipal Commission of Education of China, Open Project of State Key Laboratory of Supramolecular Structure and Materials (SKLSSM2015017), and Beijing Young Talents Plan (YETP0488).

Received: June 15, 2015
Revised: July 10, 2015
Published online: August 13, 2015

[1] W. Wang, W. T. Duan, S. Ahmed, T. E. Mallouk, A. Sen, *Nano Today* **2013**, *101*, 531.
[2] a) S. Sengupta, M. E. Ibele, A. Sen, *Angew. Chem.* **2012**, *126*, 8434; b) S. Sengupta, M. E. Ibele, A. Sen, *Angew. Chem. Int. Ed.* **2012**, *51*, 8434.
[3] W. Gao, J. Wang, *Nanoscale* **2014**, *6*, 10486.
[4] M. Sitti, *Nature* **2009**, *458*, 1121.
[5] R. Yoshida, T. Sakai, Y. Hara, S. Maeda, S. Hashimoto, D. Suzuki, Y. Murase, *J. Controlled Release* **2009**, *140*, 186.
[6] G. A. Ozin, I. Manners, S. Fournier-Bidoz, A. Arsenault, *Adv. Mater.* **2005**, *17*, 3011.
[7] B. Behkam, M. Sitti, *Appl. Phys. Lett.* **2007**, *90*, 023902.
[8] G. N. Ju, M. J. Cheng, M. Xiao, J. M. Xu, K. Pan, X. Wang, Y. J. Zhang, F. Shi, *Adv. Mater.* **2013**, *25*, 2915.
[9] L. Zhang, J. J. Abbott, L. X. Dong, K. E. Peyer, B. E. Kratochvil, H. X. Zhang, C. Bergeles, B. J. Nelson, *Nano Lett.* **2009**, *9*, 3663.
[10] a) Y. Ma, Y. Y. Zhang, B. S. Wu, W. P. Sun, Z. G. Li, J. Q. Sun, *Angew. Chem.* **2011**, *123*, 6378; b) Y. Ma, Y. Y. Zhang, B. S. Wu, W. P. Sun, Z. G. Li, J. Q. Sun, *Angew. Chem. Int. Ed.* **2011**, *50*, 6254.
[11] J. Simmchen, A. Baeza, D. Ruiz, M. J. Esplandiu, M. Vallet-Regi, *Small* **2012**, *8*, 2053.
[12] a) V. V. Singh, F. Soto, K. Kaufmann, J. Wang, *Angew. Chem.* **2015**, *127*, 7000; b) V. V. Singh, F. Soto, K. Kaufmann, J. Wang, *Angew. Chem. Int. Ed.* **2015**, *54*, 6896.
[13] M. J. Cheng, G. N. Ju, Y. W. Zhang, M. M. Song, Y. J. Zhang, F. Shi, *Small* **2014**, *10*, 3907.
[14] a) A. A. Solovev, S. Sanchez, M. Pumera, Y. F. Mei, O. G. Schmidt, *Adv. Funct. Mater.* **2010**, *20*, 2430; b) R. F. Ismagilov, A. Schwartz, N. Bowden, G. M. Whitesides, *Angew. Chem.* **2002**, *114*, 674; c) R. F. Ismagilov, A. Schwartz, N. Bowden, G. M. Whitesides, *Angew. Chem. Int. Ed.* **2002**, *41*, 652.
[15] W. F. Paxton, K. C. Kistler, C. C. Olmeda, A. Sen, S. K. St. Angelo, Y. Cao, T. E. Mallouk, P. E. Lammert, V. H. Crespi, *J. Am. Chem. Soc.* **2004**, *126*, 13424.
[16] D. Okawa, S. J. Pastine, A. Zettl, J. M. J. Fréchet, *J. Am. Chem. Soc.* **2009**, *131*, 5396.
[17] M. Xiao, C. Jiang, F. Shi, *NPG Asia Mater.* **2014**, *6*, e128.
[18] I. S. M. Khalil, V. Magdanz, S. Sanchez, O. G. Schmidt, S. Misra, *Appl. Phys. Lett.* **2013**, *103*, 172404.
[19] S. T. Chang, V. N. Paunov, D. N. Petsev, O. D. Velve, *Nat. Mater.* **2007**, *6*, 235.
[20] M. Takinoue, Y. Atsumi, K. Yoshikawa, *Appl. Phys. Lett.* **2010**, *96*, 104105.
[21] a) Z. G. Wu, T. L. Li, W. Gao, T. L. Xu, B. Jurado-Sánchez, J. X. Li, W. W. Gao, Q. He, L. F. Zhang, J. Wang, *Adv. Funct. Mater.* **2015**, *25*, 3881; b) D. Kagan, M. J. Benchimol, J. C. Claussen, E. Chuluun-Erdene, S. Esener, J. Wang, *Angew. Chem.* **2012**, *124*, 7637; c) D. Kagan, M. J. Benchimol, J. C. Claussen, E. Chuluun-Erdene, S. Esener, J. Wang, *Angew. Chem. Int. Ed.* **2012**, *51*, 7519.
[22] a) Y. Y. Hong, M. Diaz, U. M. Córdova-Figueroa, A. Sen, *Adv. Funct. Mater.* **2010**, *20*, 1568; b) Z. G. Wu, X. K. Lin, Y. J. Wu, T. Y. Si, J. M. Sun, Q. He, *ACS Nano* **2014**, *8*, 6097.
[23] T. L. Xu, F. Soto, W. Gao, V. Garcia-Gradilla, J. X. Li, X. J. Zhang, J. Wang, *J. Am. Chem. Soc.* **2014**, *136*, 8552.
[24] C. Pawashe, S. Floyd, M. Sitti, *Appl. Phys. Lett.* **2009**, *94*, 164108.
[25] a) V. Magdanz, G. Stoychev, L. Ionov, S. Sanchez, O. G. Schmidt, *Angew. Chem.* **2014**, *126*, 2711; b) V. Magdanz, G. Stoychev, L. Ionov, S. Sanchez, O. G. Schmidt, *Angew. Chem. Int. Ed.* **2014**, *53*, 2673.
[26] a) Y. J. Wu, Z. G. Wu, X. K. Lin, Q. He, J. B. Li, *ACS Nano* **2012**, *6*, 10910; b) Z. G. Wu, X. K. Lin, X. Zou, J. M. Sun, Q. He, *ACS Appl.*

Mater. Interfaces **2015**, *7*, 250; c) Z. G. Wu, Y. J. Wu, W. P. He, X. K. Lin, J. M. Sun, Q. He, *Angew. Chem.* **2013**, *125*, 7138; d) Z. G. Wu, Y. J. Wu, W. P. He, X. K. Lin, J. M. Sun, Q. He, *Angew. Chem. Int. Ed.* **2013**, *52*, 7000; e) Z. G. Wu, T. L. Li, J. X. Li, W. Gao, T. L. Xu, C. Christianson, W. W. Gao, M. Galarnyk, Q. He, L. F. Zhang, J. Wang, *ACS Nano* **2014**, *8*, 12041.

[27] M. Xiao, X. P. Guo, M. J. Cheng, G. N. Ju, Y. J. Zhang, F. Shi, *Small* **2014**, *10*, 859.

[28] H. Y. Dong, M. J. Cheng, Y. J. Zhang, H. Wei, F. Shi, *J. Mater. Chem. A* **2013**, *1*, 5886.

[29] N. Zhao, F. Shi, Z. Q. Wang, X. Zhang, *Langmuir* **2005**, *21*, 4715.

[30] M. J. Cheng, Q. Liu, G. N. Ju, Y. J. Zhang, L. Jiang, F. Shi, *Adv. Mater.* **2014**, *26*, 306.

[31] G. N. Ju, M. J. Cheng, F. Shi, *NPG Asia Mater.* **2014**, *6*, e111.

[32] F. Xia, L. Feng, S. T. Wang, T. L. Sun, W. L. Song, W. H. Jiang, L. Jiang, *Adv. Mater.* **2006**, *18*, 432.